Alterations in protein kinase A substrate specificity as a potential cause of Cushing's Syndrome

Bathon, Kerstin; Wigand, Isabel; Vanselow, Jens T.; Ronchi, Cristina; Sbiera, Silviu; Schlosser, Andreas; Calebiro, Davide; Fassnacht, Martin

DOI:
10.1210/en.2018-00775

License:
Other (please specify with Rights Statement)

Document Version
Peer reviewed version

Citation for published version (Harvard):
Bathon, K, Wigand, I, Vanselow, JT, Ronchi, C, Sbiera, S, Schlosser, A, Calebiro, D & Fassnacht, M 2019, 'Alterations in protein kinase A substrate specificity as a potential cause of Cushing's Syndrome', *Endocrinology*, vol. 160, no. 2, pp. 447-459. https://doi.org/10.1210/en.2018-00775

Alterations in Protein Kinase A Substrate Specificity as a Potential Cause of Cushing's Syndrome

Kerstin Bathon[1], Isabel Weigand[2], Jens T. Vanselow[3], Cristina L. Ronchi[2,5,6], Silviu Sbiera[2], Andreas Schlosser[3], Martin Fassnacht[2,4], Davide Calebiro[1,5,7*]

[1] Institute of Pharmacology and Toxicology and Bio-Imaging Center, University of Würzburg, 97078 Würzburg, Germany

[2] Department of Internal Medicine I, Division of Endocrinology and Diabetes, University Hospital, University of Würzburg, 97080 Würzburg, Germany

[3] Rudolf Virchow Center, University of Würzburg, 97080 Würzburg, Germany

[4] Central Laboratory, University Hospital Würzburg, 97080 Würzburg, Germany

[5] Institute of Metabolism and Systems Research (IMSR), University of Birmingham, B15 2TT Birmingham, UK

[6] Centre for Endocrinology, Diabetes and Metabolism (CEDAM), Birmingham Health Partners, B15 2TT Birmingham, UK

[7] Centre of Membrane Proteins and Receptors (COMPARE), B15 2TT Birmingham, UK

Short title: Mutations in adrenal Cushing alter PKA specificity

Keywords: PKA, Cushing's syndrome, *PRKACA* mutations

* Address correspondence and material requests to:
Davide Calebiro MD PhD DSc
Institute of Metabolism and Systems Research
College of Medical and Dental Sciences
Edgbaston
Birmingham
B15 2TT
Tel. +44 (0) 121 414 3928
Fax. +44 (0) 121 415 8712

email. davide.calebiro@toxi.uni-wuerzburg.de

Funding

This study was supported by the IZKF Würzburg (grant B-281 to D.C. and M.F.), the ERA-NET “E-Rare” (grant 01GM1407B to M.F. and D.C.) and the Deutsche Forschungsgemeinschaft (SFB/Transregio 166–Project C1 to D.C. and SFB/Transregio 205/1 to M.F.). KB was partially supported by a grant of the German Excellence Initiative to the Graduate School of Life Sciences, University of Würzburg. The tumor samples were stored at the Interdisciplinary Bank of Biomaterials and Data of the University Hospital of Würzburg and the Julius Maximilian University of Würzburg (idbw). The implementation of idbw has been supported by a grant of the Federal Ministry for Education and Research (Grant number FKZ: 01EY1102).

Disclosure Summary: The authors have nothing to disclose.

Abstract

Cushing's syndrome is a severe endocrine disorder of cortisol excess, associated with major metabolic and cardiovascular sequelae. We recently identified somatic mutations in the gene (*PRKACA*) encoding the catalytic α (Cα) subunit of protein kinase A (PKA) to be responsible for cortisol-producing adrenocortical adenomas (CPAs), which are a major cause of Cushing's syndrome. In spite of previous studies on the two initially identified mutations (L206R, 199_200insW), the mechanisms of action of the clinically highly relevant *PRKACA* mutations remain poorly understood. Here, by investigating a large panel of *PRKACA* mutations including all those identified so far in Cushing's syndrome, we unexpectedly find that not all mutations interfere with the binding of regulatory (R) subunits as previously hypothesized. Since several mutations lie in a region of PKA Cα involved in substrate recognition, we have investigated their consequences on substrate specificity by quantitative phosphoproteomics. We find that all three mutations analyzed (L206R, 200_201insV and d244-248+E249Q) cause major changes in the preference of PKA for its targets, leading to hyperphosphorylation of several PKA substrates, including most notably histone H1.4 at Ser36, which is required for and promotes mitosis. This is reflected by a 9-fold hyperphosphorylation of H1.4 in CPAs carrying the L206R mutation. Thus, our findings suggest that besides hampering binding to R subunits, *PRKACA* mutations act via altering PKA substrate specificity. These findings shed new light on the molecular events leading to Cushing's syndrome and provide an illustrative example of how mutations altering substrate specificity of a protein kinase might cause human disease.

Introduction

Cushing's syndrome is an endocrine disease characterized by cortisol excess. If not promptly recognized and treated, it is associated with severe morbidity and increased mortality, mostly due to metabolic and cardiovascular sequelae, such as diabetes mellitus, osteoporosis and hypertension (1,2). Beside ACTH-producing pituitary adenomas, cortisol-producing adenomas of the adrenal are the major cause of endogenous Cushing's syndrome (3).

Protein kinase A (PKA) is the main intracellular mediator of the ubiquitous second messenger cyclic AMP (cAMP), which is produced in response to several hormones and neurotransmitters (4,5). In its inactive state, PKA is a tetrameric complex composed of two regulatory (R) and two catalytic (C) subunits (5), which exist in different isoforms – three for C (α, β, γ) and four for R (Iα, Iβ, IIα, IIβ) subunits, each encoded by a separate gene (6). Additionally, protein kinase X (PrKX) can also form holoenzymes with R subunits (7). In the inactive complex, two short linear segments emanating from each R subunit, known as inhibitory sequences, act as substrates (RII) or pseudo-substrates (RI) that occupy the active site clefts of the C subunits, thus preventing the access of other substrates (5,8,9); this keeps PKA in the inactive state (5,8,9). Binding of cAMP to two distinct sites on each R subunit induces their dissociation from the C subunits, allowing the C subunits to phosphorylate a large number of PKA substrates located in both the cytosol and the nucleus (5,8,9).

Our group has recently discovered that somatic mutations in the gene coding for the Cα subunit of PKA (*PRKACA*) are responsible for Cushing´s syndrome due to cortisol-producing adrenocortical adenomas (CPAs) (10-13). These findings have been independently confirmed by other groups (14-18). Very recently, rare mutations in the gene coding for the Cβ subunit of PKA (*PRKACB*) have also been found in CPAs (19). Between 23 and 67% of all CPAs carry a recurrent mutation (L206R) of a residue in the Cα subunit that is involved in the interaction with the R subunits (10,11,14-16). By screening a large group of CPAs, we

have in the meantime identified six additional *PRKACA* mutations (199_200insW, S213R+insIILR, 200_201insV, W197R, d244-248+E249Q and E32V) in unilateral adenomas of patients affected by overt Cushing's syndrome (10-12). With one exception (E32V), all identified mutations lie in a hot spot region on the surface of the Cα subunit that is adjacent to the active site cleft and faces the R subunit (12).

Whereas all previous studies provide strong evidence for a causal role of *PRKACA* mutations, the mechanisms linking these mutations to increased cell proliferation and cortisol secretion in adrenocortical cells are still debated (10,14-16). One of the initial studies suggested that the L206R mutation increases PKA activity by enhancing substrate interaction and/or the catalytic activity of the enzyme (14). In contrast, two other studies suggested that the L206R mutation might prevent binding of the R subunit (15,16). In strong support of this possibility, we subsequently demonstrated that the two initially identified mutations (L206R and 199_200insW) interfere with the formation of a stable complex with R subunits, thus rendering mutated Cα subunits constitutively active (13). However, we did not observe increased catalytic activity (13). Whereas these data indicate that a reduced interaction with R subunits is likely involved in the pathogenesis of Cushing's syndrome – at least in the case of the two investigated *PRKACA* mutations (L206R and 199_200insW) – additional mechanisms might play an equally important role.

Here, we report a comprehensive functional characterization of all *PRKACA* mutations identified so far. Unexpectedly, our results indicate that besides interfering with the binding of R subunits, *PRKACA* mutations cause major changes in the preference of PKA for its targets, leading to hyperphosphorylation of several PKA substrates, including most notably histone H1.4 at Ser36, which is required for and promotes mitosis (20).

Methods

Plasmids

Plasmids encoding human RIα, RIIβ and RIIβ-FLAG were described earlier (13). A plasmid encoding human wild-type Cα was purchased from Origene. Mutations in the coding sequence of Cα were introduced by PCR as previously described (10). To generate a plasmid encoding a FLAG-tagged RIα subunit, a fragment containing the entire coding sequence of the human RIα subunit was amplified by PCR with a forward primer containing the FLAG tag (amino-acid sequence DYKDDDDA) and a HindIII site at the 5' and a reverse primer containing a NotI site at the 3'. This fragment was subsequently cloned between the HindIII and NotI sites of pcDNA3.

Tumor tissue

A total of 8 snap-frozen tumor specimens from CPAs were investigated. All samples were collected at the University Hospital of Würzburg. Six of these samples had been included in previous reports from our group: three in Ronchi et al. (12) and three in Beuschlein et al. (10). According to our previous sequencing data, four CPA samples harbored somatic *PRKACA* mutations. In particular, three samples from patients with overt Cushing´s syndrome presented a L206R substitution and one sample from a patient with mild autonomous cortisol secretion (subclinical Cushing´s syndrome) presented a d244-248+E249Q mutation. The four remaining CPAs were *PRKACA* wild-type. The collection of the clinical data and the biomaterial for this retrospective study was approved by the ethics committee of the University of Würzburg (approvals no. 93/02 and 88/11). Written informed consent was obtained from all patients.

Cell culture and transfection

HEK293A cells were obtained from ATCC. Cells were cultured in Dulbecco´s modified Eagle's medium (DMEM) supplemented with 10% FCS, 0.1 mg/ml streptomycin and 100

U/ml penicillin at 37 °C, 5% (vol/vol) CO_2. HEK293A cells were seeded at a density of $3.5x10^6$ cells/15-cm Petri dish, 1.2 x 10^6 cells/10-cm Petri dish or 0.25 x 10^6 cells/well onto 6-well plates and allowed to grow for 24 h, after which they were transfected with the Effectene transfection kit (Qiagen) according to the manufacturer´s protocol. A 1:8 ratio of transfected C and R subunit DNAs was used to favor association between C and R subunits (10). All experiments were performed 48 h after transfection. For SILAC labeling, the cells were grown in light (Lys0, Arg0) or heavy (Lys8, Arg10) labeled DMEM supplemented with 10% dialyzed FCS and 0.1 mg/ml streptomycin and 100 U/ml penicillin for at least 6 passages before the experiment.

Preparation of cell lysates

Cells were washed with ice-cold phosphate-buffered saline (PBS), scraped off plates, and resuspended in 300 μl 5/2 buffer (5 mM Tris-HCl, 2 mM EDTA, pH 7.4). Thereafter, samples were homogenized using an Ultraturrax device for 20 s on ice and centrifuged at 50,000 x *g* for 30 min at 4 °C to remove membranes.

Preparation of total cell lysates

Cells were washed once with PBS. Then, 2 ml of lysis buffer (8M urea, 1 mM sodium vanadate, 2.5 mM pyrophosphate, 1 mM β-glycerophosphate, 20mM HEPES, pH 8.0) supplemented with the cOmplete Mini EDTA-free protease inhibitor cocktail (Roche) were added to each 15-cm Petri dish and the cells were scraped into the buffer. Cell suspensions were sonicated three times for 15 sec each and lysates were cleared by centrifugation at 4,000 rpm for 1 h at 15 °C.

PKA activity assay

PKA catalytic activity was measured on cell lysates using the PepTag non-radioactive cAMP-dependent protein kinase assay (Promega), which uses fluorescent kemptide as a

substrate, following the manufacturer´s instructions. Images of the gels were acquired with a gel documentation system (Herolab) and analyzed using the ImageJ software (http://rsbweb.nih.gov/ij). Endogenous PKA activity was subtracted and values were normalized to the value of the stimulated wild-type.

Co-immunoprecipitation

Cells were lysed with a buffer containing 150 mM NaCl, 1 mM EDTA, 1 mM EGTA, 1% Triton X-100, 20 mM Tris-HCl, pH 7.5, supplemented with cOmplete Mini protease inhibitor cocktail (Roche). Lysates were centrifuged at 20,000 x *g* for 10 min at 4 °C. Supernatants were transferred to a new vial and incubated with protein-A sepharose for 2 h at 4 °C under continuous rotation. Protein-A sepharose was preincubated with a mouse monoclonal anti-FLAG antibody (Sigma-Aldrich, # F3165). Preincubations were performed overnight at 4 °C under continuous rotation. After the incubation of protein-A sepharose with the cell lysates, samples were washed 5 times with lysis buffer. Proteins were recovered from protein-A sepharose by addition of Laemmli buffer, followed by incubation at 95 °C for 3 min. After Western blot analysis and quantification, the amount of Cα was normalized to that in the wild-type sample.

Histone extraction

Histones were acid-extracted from cells and CPA samples as described by Shechter et al. (21). Briefly, harvested cells or Douncer-homogenized tissue samples were lysed in a hypotonic lysis buffer (150 mM Tris/HCl, 1 mM KCl, 1.5 mM $MgCl_2$, 1 mM DTT, pH 8.0) supplemented with 0.5 µg/ml leupeptin, 2 µg/ml aprotinin, 0.1 mM phenylmethylsulfonyl fluoride (PMSF), the cOmplete Mini protease inhibitor cocktail (Roche) and a phosphatase inhibitor cocktail (Roche). Lysates were then acid-extracted with H_2SO_4 for 30 min followed by precipitation with trichloroacetic acid and resuspension in H_2O.

Western blot analysis

Samples were mixed with Laemmli buffer and incubated at 95 °C for 3 min. Proteins were separated by electrophoresis on either a 10% or 15% (for histone H1.4) SDS polyacrylamide gel and electro-transferred to a PVDF membrane (Merck Millipore). Membranes were blocked with Tris-buffered saline supplemented with 1% Tween and 5% skim milk powder or bovine serum albumin (antibodies detecting phosphoproteins) for 1 hour at RT, and incubated overnight at 4 °C with the indicated primary antibody, followed by incubation with horseradish peroxidase-conjugated secondary antibodies for 1 h at RT. PKA Cα subunits were detected with a rabbit polyclonal antibody (Cell Signaling #4782, 1:7,000 dilution). FLAG-tagged R subunits were detected using a rabbit monoclonal anti-FLAG antibody (Sigma-Aldrich, #F7425, 1:4,000 dilution). PKA RIα subunits were detected using a mouse monoclonal antibody (BD Transduction Lab., #610609, 1:1,000 dilution) and RIIβ subunits with a mouse monoclonal antibody (BD Transduction Lab., #610625, 1:2,000 dilution). Phosphorylated PKA substrates were detected using a rabbit polyclonal antibody (Cell Signaling, #9621, 1:1,000 dilution). A rabbit polyclonal antibody (ThermoFisher, #PA5-31908, 1:2,000 dilution) and a rabbit polyclonal antibody (ThermoFisher, #PA5-31907, 1:1,000 dilution) was used for total histone H1.4 and Ser36 phosphorylated histone H1.4, respectively.

Substrate specificity of PKA Cα mutants *in silico*

The *in silico* prediction was done using the Kinase Substrate Prediction v 2.0 algorithm (22). This algorithm predicts substrate specificity based on the primary amino acid sequence of more than 488 human protein kinase catalytic domains and 10,000 known kinase–substrate phosphosite pairs. The algorithm computes a specificity matrix for a given kinase, or mutant thereof, where values indicate the relative preference for each amino acid at each position around the phosphoacceptor site. Only relevant changes are reported.

Substrate specificity of PKA Cα mutants *in vitro*

Mutant and wild-type samples were labelled with heavy and light amino acids as described in cell culture and transfection. Before preparing total cell lysates, the cells were stimulated with 10 μM forskolin for 30 min. Protein concentration of the total cell lysates were determined using the BCA assay. Before processing the samples for phosphoproteomics, an input sample for proteome analysis was taken, which was digested with trypsin and analysed by nano LC-MS/MS. For phosphoproteomics experiments, no more than 20 mg protein were used. Substrate specificity was assessed using the PTMScan Phospho-PKA Substrate Motif (RRXS*/T*) Kit (Cell Signaling, #5565) following the manufacturer´s instructions – see Supplementary Data (23) for details. The dried peptides were stored at -20°C until the nano LC-MS/MS analysis.

Nano LC-MS/MS analysis

Nanoscale liquid chromatography coupled to tandem mass spectrometry (nano LC-MS/MS) analyses were performed on an Orbitrap Fusion system (Thermo Scientific) equipped with an EASY-Spray Ion Source and coupled to an EASY-nLC 1000 (Thermo Scientific). Peptides, resuspended in 2% acetonitrile and 0.1% formic acid, were loaded on a trapping column (2 cm x 75 µm ID, PepMap C18, 3 µm particles, 100 Å pore size) and separated on an EASY-Spray column (50 cm x 75 µm ID, PepMap C18, 2 µm particles, 100 Å pore size) with a 140-min linear gradient from 3% to 45% acetonitrile and 0.1 % formic acid.

Both MS and MS/MS scans were acquired on the Orbitrap analyzer with a resolution of 60,000 for MS scans and 15,000 for MS/MS scans. HCD fragmentation with 35% normalized collision energy was applied. A Top Speed data-dependent MS/MS method with a fixed cycle time of 3 s was used. Dynamic exclusion was applied with a repeat count of 1 and an exclusion duration of 60 s; singly charged precursors were excluded from selection. Minimum signal threshold for precursor selection was set to 5×10^4. Predictive AGC was

used with AGC target values of 2 x 10^5 for MS scans and 5 x 10^4 for MS/MS scans. EASY-IC was used for internal calibration.

Raw data processing and database search

For raw-data processing, database searches and SILAC quantification, the MaxQuant software version 1.5.6.5 was used (24). The search was performed against the human UniProt reference proteome database (download date: 2016-12-09) plus a small database containing known immunoglobulin chains. Additionally, a database containing common contaminants (included in MaxQuant) was used. The search was performed with tryptic cleavage specificity and 3 allowed miscleavages. Results were filtered to a false-discovery rate (FDR) <1% on protein, peptide and phosphosite level and for modified peptides a minimum score of 40 and a minimum delta score of 6 were required. In addition to default settings, protein N-terminal acetylation, Gln to pyro-Glu formation (N-term. Q), oxidation (M) and phosphorylation (STY) were included as variable modifications; carbamidomethyl (C) was set as fixed modification. For SILAC quantification, light (Arg0/Lys0) and heavy (Arg10/Lys8) labeling were selected, with max. 4 labeled amino acids per peptide allowed; matching between runs was disabled.

For further data analysis in R, the MaxQuant “Phospho (STY) Sites” table was processed, and only phosphosites with a localization probability >0.75 and a PEP < 0.05 have been included. For each experiment, the distribution of log2-transformed heavy/light SILAC ratios were normalized to the first mode of the distribution. Data from replicate experiments were combined, and Student´s t-test as well as limma p-values were calculated and corrected for multiple-hypothesis testing (Benjamini-Hochberg algorithm, FDR). In addition, boxplot outliers with values outside of the 1.5x and/or the 3x interquartile range (IQR) of the 1st or 3rd quartile (Q1 or Q3) were labeled as significant or highly significant, only if a replicate notch, defined as 1.58*IQR/sqrt(number of experiments), was not overlapping with the median of all such notches.

Motif logo

For calculation of position weight matrices from the phosphoproteomics data, the web tool plogo (http://plogo.uconn.edu/) (25) was used. Values were calculated relative to the background amino acid frequencies in the human proteome. Motif logos were then generated using the Weblogo software version 3.5.0 (26).

Structures

Protein structures were generated using PyMol version 1.7.4.5. PDB entries 3TNP (9) and 3TNQ (9) were used as templates for the structures of the PKA Cα -RIIβ holoenzyme and the Cα subunit in complex with a phosphorylated substrate, respectively.

Statistical analyses

Statistical analyses were performed using the Prism 6 software (GraphPad). Values are given as mean ± s.e.m. Differences between two groups were assessed by two-tailed Student's t-test. Differences among three or more groups were assessed by two-way analysis of variance (ANOVA), followed by Bonferroni's post hoc test. Differences were considered significant for P values < 0.05.

Results

PRKACA mutations have variable effects on R subunit binding

Through genetic screening of a large series of CPAs from patients with Cushing´s syndrome, we have identified a total of 7 *PRKACA* mutations, including the most frequent L206R, with an overall prevalence in CPAs of about 40% (10-12). The results of all available studies to date are summarized in Table 1. With the exception of E32V, all mutations identified so far lie at a hot spot at the interface with the R subunit (Fig. 1). Since our previous data indicated that the two initially identified mutations (L206R and 199_200insW) interfere with the formation of a stable complex with the inhibitory RIIβ subunit (13), we first evaluated the interaction of all mutations identified so far with both RIα and RIIβ – the two main R subunit isoforms expressed in adrenocortical cells – by co-immunoprecipitation (Fig. 2 and Supplementary Data, Fig. S1 (23)).

As expected, we observed a robust co-immunoprecipitation of exogenously expressed wild-type Cα with both RIα and RIIβ (Fig. 2 and Supplementary Data, Fig. S1 (23)). In the case of four mutants (199_200insW, L206R, 200_201_insV and S213R+insIILR), we detected only faint signals in the presence of either RIα or RIIβ, indicating that the interaction with both R subunit isoforms was largely lost, consistent with our previous observations (13). Unexpectedly, however, two mutants (W197R and E32V) displayed normal binding to both RIα and RIIβ (Fig. 2, arrows). Of note, a previous report indicates that the W197R mutant cannot bind to R subunits unless they are stripped off of cAMP, a condition that is not occurring in intact cells (27). The d244-248+E249Q mutant had an interesting behavior as it showed normal binding to RIIβ but a complete lack of binding to RIα (Fig 2, arrow). With the exception of S213R+insIILR, all Cα mutants dissociated virtually completely from R subunits upon addition of cAMP (Fig. 2 and Supplementary Data, Fig. S1 (23)).

PRKACA mutations have variable effects on PKA activity

Next, we investigated the activity of the Cα mutants against the widely used synthetic peptide substrate kemptide. In lysates obtained from HEK293A cells co-transfected with wild-type or mutant Cα subunits and either RIα or RIIβ, we observed a high variability among the investigated Cα mutants. A first group of mutants (199_200insW, L206R, W197R, d244-248+E249Q and S213R+insIILR) was characterized by increased basal activity against kemptide at least in one condition (i.e. with RIα or RIIβ) (Fig. 3). The E32V mutant was apparently behaving like wild-type Cα (Fig. 3). The 200_201insV mutant was characterized by a strongly reduced maximal activity (measured in the presence of cAMP) against kemptide compared to wild-type Cα (Fig. 3).

Unexpectedly, a different picture was observed when PKA activity was evaluated against endogenous substrates in lysates of HEK293A cells transfected with the different Cα mutants and analyzed by Western blot analysis with an anti-phospho-PKA substrate antibody (Supplementary Data, Fig. S2 (23)). In this assay, RIIβ but not RIα co-expression was capable of buffering the activity of exogenous wild-type or mutant Cα subunits, consistent with previous observations (9). Therefore, we focused on the results obtained in the presence of RIIβ. In cells co-transfected with RIIβ, two Cα mutants (199_200insW and L206R) showed strongly increased basal activity compared to wild-type Cα (Supplementary Data, Fig. S2 (23)). The remaining mutants were characterized by a variable degree of increased basal activity compared to wild-type Cα (Supplementary Data, Fig. S2 (23)). Notably, in this assay, the 200_201insV mutant, which was characterized by a strongly reduced maximal activity in the kemptide assay, could be stimulated by addition of the adenylyl cyclase activator forskolin to a similar although slightly lower extent compared to wild-type Cα (Supplementary Data, Fig. S2 (23)). At a closer look, this analysis also revealed potentially different phosphorylation patterns for the Cα mutants compared to wild-type Cα as well as among the Cα mutants (Supplementary Data, Fig. S2A, arrows (23)). Altogether, these data suggested the possibility that the investigated *PRKACA* mutations

might alter the relative preference of PKA for its substrates, so that investigating a single synthetic substrate does not provide a satisfactory description of the activity of Cα mutants against endogenous substrates.

In silico analysis of *PRKACA* mutations predicts changes in substrate specificity

Our results suggested the possibility that *PRKACA* mutations might alter the preference of PKA for its substrates and, thus, cause a relative change in substrate specificity. This hypothesis was consistent with the location of most *PRKACA* mutations in a region of Cα that is critical for substrate binding and recognition (27,28) (Fig. 1B). To further explore this possibility, we performed an *in silico* analysis using a protein kinase substrate prediction algorithm (22). The algorithm predicted relevant changes in substrate specificity for four mutants: 199_200insW, L206R, d244-248+E249Q and 200_201insV (Fig. 1B and Supplementary Data, Fig. S3 (23)). The largest change was predicted for the d244-248+E249Q mutant. For the S213R+insIILR mutant, the algorithm predicted only minor effects on substrate specificity, whereas no changes were predicted for the two remaining mutants (E32V, W197R).

Phosphoproteomics reveals major changes in substrate specificity caused by *PRKACA* mutations

Motivated by the results of the Western blot analysis and the *in silico* prediction, we used a quantitative phosphoproteomics approach to comprehensively analyze and quantitatively compare the substrate repertoires of wild-type and mutant PKA Cα in mammalian cells. The three PKA Cα mutations predicted to have the largest effects on substrate specificity were analyzed (Fig. 4). These included the frequent L206R mutation, the d244-248+E249Q mutation, which was predicted to have the strongest effect on substrate specificity, and the 200_201insV mutation, which shared prediction with the adjacent 199_200insW mutation. All cell lysates were obtained after 30-min stimulation with the adenylyl cyclase activator

forskolin to allow comparison under conditions of maximal PKA activity. The phosphoproteomics analysis identified 463 sites phosphorylated by the wild-type Cα subunit. A direct quantitative comparison between wild-type and mutant Cα subunits demonstrated that the investigated *PRKACA* mutations caused major changes in the pattern of PKA substrate phosphorylation (Fig. 4). These changes involved 62, 116 and 75 substrates that were either hyper- or hypophosphorylated by the L206R, d244-248+E249Q and 200_201insV mutants, respectively, compared to wild-type (Fig. 4 and Supplementary Data, Dataset S1 (23)). Our data also allowed us to compute sequence logos of the region encompassing the phosphoacceptor site, where the size of the letters, each corresponding to a given amino acid, indicates their relative frequency at a given position (Fig. 4). Overall, the analysis showed relevant changes in the preferred amino acids surrounding the RR/KXpS/T phosphorylation consensus sequence, including an increased preference for amino acids with small or hydrophobic, non-aromatic side chains (glycine, alanine, valine, methionine) at position +1 from the phosphoacceptor site, at the expense of phenylalanine and other amino acids (Fig. 4). Moreover, we observed an increased preference for leucine at position +1 from the phosphoacceptor site and an increased preference for acidic residues in the residues downstream of the phosphoacceptor site for the L206R mutant, consistent with a recent report by Lubner *et al.* in *E. coli* (29). Additionally, the L206R mutant was characterized by a loss of preference for arginine residues at positions -7 to -4 relative to the phosphoacceptor site and an increased preference for glutamic acid and serine at several positions. For the d244-248+E249Q mutant, we found an increased preference for leucine at position -1 from the phosphoacceptor site and a reduced preference for acidic residues downstream of the phosphoacceptor site. The latter trend was mirrored in the hypophosphorylated peptides, where acidic residues were overrepresented downstream of the phosphoacceptor site. Interestingly, both mutants (L206R and d244-248+E249Q) showed an asymmetric effect on substrate phosphorylation with a higher number of peptides that were hyperphosphorylated (40 and 93, respectively) compared to a relatively lower

number of hypophosphorylated ones (22 and 23, respectively). Therefore, both mutations mainly seemed to increase the phosphorylation of poor substrates of the wild-type enzyme, while causing only smaller decreases in the phosphorylation of other substrates. For the 200_201insV mutant, we observed an increased preference for leucine and alanine at position -1, accompanied by a loss of preference for acidic residues downstream of the phosphoacceptor site and an increased preference for proline at position +3. The loss of preference for peptides containing acidic residues at downstream positions was reflected by their relative overrepresentation in the corresponding hypophosphorylated peptides (left panel). In contrast to the other two mutants, the 200_201insV mutant was characterized by a rather symmetric distribution with 35 hypo- and 40 hyperphosphorylated peptides, suggesting that comparable numbers of substrates were either hyper- or hypophosphorylated. In general, the phosphorylation patterns differed among the three Cα mutants. However, four substrates were consistently found to be hyperphosphorylated by all three mutants compared to wild type. These were the citron rho-interacting kinase (CIT; Ser 480), the mitochondrial import receptor subunit TOM34 (Ser 93), histone H1.2 (Ser 36) and histone H1.4 (Ser 36) (Fig. 4). H1.2, H1.4, TOM34 and CIT were also found to be present and phosphorylated at the same sites in lysates of the cortisol-producing adrenocortical cell line NCI-H295R (Supplementary Data, Dataset S1 (23)).

To rule out that the observed changes were due to changes in protein levels rather than phosphorylation, we performed an additional proteomics experiment on the same cell lysates, which allowed us to directly compare the relative amounts of proteins at the proteome level between wild-type and mutant samples, including, importantly, H1.2, H1.4 and TOMM34 (Supplementary Data, Fig. S4, Dataset S2 (23)). The results indicate that the levels of most proteins, including H1.2, H1.4 and TOMM34, were unchanged between wild-type and mutant samples.

Whereas hyperphosphorylation of CIT and TOM34 might mediate some effects of *PRKACA* mutations, we concentrated our attention on H1 because phosphorylation by PKA of histone

H1.4 on Ser36 – and possibly of the highly homologous Ser36 site on H1.2 – is required for mitosis (20).

PRKACA mutations cause histone H1.4 hyperphosphorylation *in vitro* and in CPAs

The conserved Ser36 phosphorylation site on histone H1 isoforms has been implicated in chromatin condensation and mitosis (20). This has been better studied for histone H1.4, which has been shown to be phosphorylated by PKA on Ser36 during mitosis, an event that has been demonstrated to induce histone H1.4 dissociation from chromatin and be required for mitosis (20). Because of the potential relevance of histone H1 Ser36 phosphorylation for the mechanism of action of *PRKACA* mutations, we first investigated histone H1.4 phosphorylation in HEK293A cells transfected with Cα subunit mutants. In HEK293A cells, overexpression of the L206R mutant caused a strong increase (12-fold under basal conditions; 3-fold in the presence of forskolin) in histone H1.4 Ser36 phosphorylation compared to overexpression of wild-type Cα (Fig. 5 and Supplementary Data, Fig. S5 (23)). Modestly increased levels of histone H1.4 Ser36 phosphorylation were also observed with the d244-248+E249Q and 200_201insV mutants compared with wild-type Cα, even though these differences did not reach statistical significance (Fig. 5 and Supplementary Data, Fig. S5 (23)).

Furthermore, we analyzed histone H1.4 Ser36 phosphorylation in human CPA tumor samples of patients with Cushing´s syndrome with or without *PRKACA* mutations (summary of clinical data in Supplementary Data, Table S1 (23)). Importantly, a 9-fold increase in histone H1.4 Ser36 phosphorylation was observed in CPAs carrying the L206R mutation compared with CPAs without *PRKACA* mutations (1.9±0.26 vs. 0.21±0.29, p=0.009) (Fig. 6). These results indicated that in patients with adrenal Cushing´s syndrome, at least the by far most frequent L206R mutation is associated with a strong increase of H1.4 phosphorylation in the patients´ tumor tissue.

Discussion

Our results indicate that *PRKACA* mutations found in CPAs alter PKA preference for its targets, inducing hyperphosphorylation of several PKA substrates, including most notably histone H1.4 at Ser36, which has been suggested to play an essential role in mitosis (20). Thus, our study reveals another key mechanism that, together with increased PKA basal activity, might explain the development of CPAs in the presence of somatic *PRKACA* mutations (Supplementary Data, Fig. S6 (23)).

Whereas our previous study on the two *PRKACA* mutations intially identified in adrenal Cushing´s syndrome (L206R and 199_200insW) showed that these mutations increase basal PKA activity by preventing the binding of R subunits, the present results obtained on a larger group of *PRKACA* mutations indicate that this is not always the case (see Supplementary Data, Fig. S7 (23) for a summary of the present results), and that a relative change in PKA substrate specificity likely contributes to the mechanism of action of *PRKACA* mutations.

Our phosphoproteomics analysis revealed four PKA subtrates that were hyperphosphorylated by all three PKA Cα mutants analyzed, and, thus, are potentially involved in the pathogenesis of CPAs due to *PRKACA* mutations. These included CIT (Ser 480), TOM34 (Ser 93), histone H1.2 (Ser 36) and histone H1.4 (Ser 36). Importantly, all four substrates were also identified to be expressed and phosphorylated on the same sites in lysates of NCI-H295R cells, which are widely used as a model of differentiated, cortisol-producing adrenocortical cells (Supplementary Data, Dataset S1 (23)). Of these, histone H1.4 and the highly homologous histone H1.2 appeared particularly intriguing because H1 histones play an important role in promoting, regulating and maintaining chromatin organization and, thus, are deeply involved in the regulation of gene transcription and mitosis (20,30-32). H1 histones possess a conserved serine residue at position 36 (Ser36), which has been mainly investigated for histone H1.4. Interestingly, histone H1.4 has been shown to be strongly phosphorylated on Ser36 by PKA at the first stage of mitosis

(prophase), to then rapidly revert to normal, low phosphorylation levels during cytokinesis (20). Phosphorylation of histone H1.4 on Ser36 has been shown to promote histone H1.4 dissociation from mitogenic DNA and induce changes in chromatin organization (20). Moreover, it has been shown that silencing H1.4 inhibits mitosis, an effect that cannot be rescued by a phosphorylation-deficient H1.4 mutant (S36A) (20). These findings indicate that the PKA-dependent phosphorylation of histone H1.4 at Ser36 plays an important role in promoting mitosis, presumably by inducing changes in chromatin structure that are required for the realization of the mitogenic program (20). Whereas other changes in the PKA phosphorylation pattern caused by *PRKACA* mutations might also play a role in the pathogenesis of CPAs, it is noteworthy that two of the four hyperphosphorylated sites shared by the three tested Cα mutants are Ser36 on histone H1.4 and the corresponding Ser36 on histone H1.2, which likely plays a similar role. Our finding that histone H1.4 is highly hyperphosphorylated in CPAs carrying the L206R mutation – but not in those with wild-type PKA – supports a role of H1.4 hyperphosphorylation in the pathogenesis of CPAs due to *PRKACA* mutations. Further investigations, such as studies on chromatin organization by DAPI staining and H1.4–chromatin association by immunofluorescence (20) or chromatin immunoprecipitation will be required to further clarify the impact of the increased H1.4 (Ser36) phosphorylation on chromatin organization in *PRKACA* mutated CPA tissue.

In addition to hyperphosphorylation of histone H1, that of CIT and of TOM34 – which, to the best of our knowledge, have not been previously reported to be phosphorylated by PKA – might also play a role in the mechanism of action of *PRKACA* mutations. CIT is a serine/threonine-protein kinase that has been shown to be required for cytokinesis (33). Phosphorylation of Ser480 might potentially influence the activity of CIT and, thus, affect cytokinesis. TOM34 is involved in mitochondrial protein import (34). Interestingly, yeast TOM70 has been shown to be phosphorylated by PKA on Ser174 (35), which is homologous to Ser93 in human TOM34. In yeast, TOM70 phosphorylation by PKA inhibits its receptor activity, which results in reduced mitochondrial import of metabolite carriers (35).

Phosphorylation of TOM34 at Ser93 could have a similar effect. Future studies will be required to evaluate the role of CIT and TOM34 in the pathogenesis of CPAs.

The finding that *PRKACA* mutations cause histone H1.4 phosphorylation might help explaining why these mutations lead to the development of CPAs, while normal cAMP/PKA signaling such as resulting from physiological stimulation by the adrenocorticotropic hormone (ACTH) has no or at most only mild proliferative effects on adrenocortical cells (36,37). Intriguingly, this may suggest that whereas an increase in PKA activity might be sufficient to induce excess cortisol production in the presence of *PRKACA* mutations, a change in PKA substrate preference – and the resulting hyperphosphorylation of histone H1.4 and possibly other targets involved in the control of cell replication – might be required to stimulate cell proliferation.

Finally, our findings indicate that, given the important changes in substrate specificity caused by *PRKACA* mutations, it might be possible to develop selective orthosteric PKA inhibitors that bind only to the mutant Cα subunits and, thus, selectively inhibit the mutated PKA in CPAs without affecting the function of wild-type PKA in normal cells.

In summary, our findings indicate that *PRKACA* mutations found in CPAs lead to a change in the pattern of PKA phosphorylation, which might play an important role in their mechanism of action. This not only reveals a novel key mechanism potentially involved in the pathogenesis of CPAs and Cushing's syndrome, but might also allow the development of selective PKA inhibitors for therapeutic purposes that block mutated but not wild-type PKA. Moreover, these findings provide a highly illustrative example of how mutations altering substrate specificity of a protein kinase might cause a human disease, which might also have implications for other conditions.

Author Contribution

D.C. designed research with contributions from M.F. and A.S. K.B., I.W. and J.W. performed research. K.B., I.W. and J.W. analyzed data. M.F., C.L.R. and S.S. provided tumor samples together with clinical and genetic data. K.B. and D.C. wrote the paper with contributions from M.F., A.S., I.W., C.L.R. and S.S.

Acknowledgments

We thank Bianca Klüpfel for excellent technical support and Ulrike Zabel for help with cloning.

References

1. Calebiro D, Di Dalmazi G, Bathon K, Ronchi CL, Beuschlein F. cAMP signaling in cortisol-producing adrenal adenoma. Eur J Endocrinol 2015; 173:M99-106
2. Arnaldi G, Mancini T, Tirabassi G, Trementino L, Boscaro M. Advances in the epidemiology, pathogenesis, and management of Cushing's syndrome complications. J Endocrinol Invest 2012; 35:434-448
3. Fassnacht M, Arlt W, Bancos I, Dralle H, Newell-Price J, Sahdev A, Tabarin A, Terzolo M, Tsagarakis S, Dekkers OM. Management of adrenal incidentalomas: European Society of Endocrinology Clinical Practice Guideline in collaboration with the European Network for the Study of Adrenal Tumors. Eur J Endocrinol 2016; 175:G1-G34
4. Pierce KL, Premont RT, Lefkowitz RJ. Seven-transmembrane receptors. Nat Rev Mol Cell Biol 2002; 3:639-650
5. Taylor SS, Ilouz R, Zhang P, Kornev AP. Assembly of allosteric macromolecular switches: lessons from PKA. Nat Rev Mol Cell Biol 2012; 13:646-658
6. Søberg K, Jahnsen T, Rognes T, Skålhegg BS, Laerdahl JK. Evolutionary Paths of the cAMP-Dependent Protein Kinase (PKA) Catalytic Subunits. PLoS ONE 2013; 8:e60935
7. Diskar M, Zenn H-M, Kaupisch A, Kaufholz M, Brockmeyer S, Sohmen D, Berrera M, Zaccolo M, Boshart M, Herberg FW, Prinz A. Regulation of cAMP-dependent Protein Kinases: The human protein kinase X (PrKX) reveals the role of the catalytic subunit αH-αI loop. J Biol Chem 2010; 285:35910-35918
8. Taylor SS, Buechler JA, Yonemoto W. cAMP-dependent protein kinase: framework for a diverse family of regulatory enzymes. Annu Rev Biochem 1990; 59:971-1005
9. Zhang P, Smith-Nguyen EV, Keshwani MM, Deal MS, Kornev AP, Taylor SS. Structure and Allostery of the PKA RIIβ Tetrameric Holoenzyme. Science 2012; 335:712-716

524 10. Beuschlein F, Fassnacht M, Assie G, Calebiro D, Stratakis CA, Osswald A, Ronchi
525 CL, Wieland T, Sbiera S, Faucz FR, Schaak K, Schmittfull A, Schwarzmayr T,
526 Barreau O, Vezzosi D, Rizk-Rabin M, Zabel U, Szarek E, Salpea P, Forlino A, Vetro
527 A, Zuffardi O, Kisker C, Diener S, Meitinger T, Lohse MJ, Reincke M, Bertherat J,
528 Strom TM, Allolio B. Constitutive activation of PKA catalytic subunit in adrenal
529 Cushing's syndrome. N Engl J Med 2014; 370:1019-1028
530 11. Di Dalmazi G, Kisker C, Calebiro D, Mannelli M, Canu L, Arnaldi G, Quinkler M,
531 Rayes N, Tabarin A, Laure Jullie M, Mantero F, Rubin B, Waldmann J, Bartsch DK,
532 Pasquali R, Lohse M, Allolio B, Fassnacht M, Beuschlein F, Reincke M. Novel
533 somatic mutations in the catalytic subunit of the protein kinase A as a cause of
534 adrenal Cushing's syndrome: a European multicentric study. J Clin Endocrinol Metab
535 2014; 99:E2093-2100
536 12. Ronchi CL, Dalmazi GD, Faillot S, Sbiera S, Assié G, Weigand I, Calebiro D,
537 Schwarzmayr T, Appenzeller S, Rubin B, Waldmann J, Scaroni C, Bartsch DK,
538 Mantero F, Mannelli M, Kastelan D, Chiodini I, Bertherat J, Reincke M, Strom TM,
539 Fassnacht M, Beuschlein F. Genetic Landscape of Sporadic Unilateral Adrenocortical
540 Adenomas Without *PRKACA* p.Leu206Arg Mutation. J Clin Endocrinol Metab 2016;
541 101:3526-3538
542 13. Calebiro D, Hannawacker A, Lyga S, Bathon K, Zabel U, Ronchi C, Beuschlein F,
543 Reincke M, Lorenz K, Allolio B, Kisker C, Fassnacht M, Lohse MJ. PKA catalytic
544 subunit mutations in adrenocortical Cushing’s adenoma impair association with the
545 regulatory subunit. Nat Commun 2014; 5:5680
546 14. Cao Y, He M, Gao Z, Peng Y, Li Y, Li L, Zhou W, Li X, Zhong X, Lei Y, Su T, Wang
547 H, Jiang Y, Yang L, Wei W, Yang X, Jiang X, Liu L, He J, Ye J, Wei Q, Li Y, Wang W,
548 Wang J, Ning G. Activating hotspot L205R mutation in *PRKACA* and adrenal
549 Cushing’s syndrome. Science 2014; 344:913-917

15. Goh G, Scholl UI, Healy JM, Choi M, Prasad ML, Nelson-Williams C, Kunstman JW, Korah R, Suttorp A-C, Dietrich D, Haase M, Willenberg HS, Stalberg P, Hellman P, Akerstrom G, Bjorklund P, Carling T, Lifton RP. Recurrent activating mutation in *PRKACA* in cortisol-producing adrenal tumors. Nat Genet 2014; 46:613-617

16. Sato Y, Maekawa S, Ishii R, Sanada M, Morikawa T, Shiraishi Y, Yoshida K, Nagata Y, Sato-Otsubo A, Yoshizato T, Suzuki H, Shiozawa Y, Kataoka K, Kon A, Aoki K, Chiba K, Tanaka H, Kume H, Miyano S, Fukayama M, Nureki O, Homma Y, Ogawa S. Recurrent somatic mutations underlie corticotropin-independent Cushing's syndrome. Science 2014; 344:917-920

17. Nakajima Y, Okamura T, Gohko T, Satoh T, Hashimoto K, Shibusawa N, Ozawa A, Ishii S, Tomaru T, Horiguchi K, Okada S, Takata D, Rokutanda N, Horiguchi J, Tsushima Y, Oyama T, Takeyoshi I, Yamada M. Somatic mutations of the catalytic subunit of cyclic AMP-dependent protein kinase (*PRKACA*) gene in Japanese patients with several adrenal adenomas secreting cortisol [Rapid Communication]. Endocr J 2014; 61:825-832

18. Thiel A, Reis A-C, Haase M, Goh G, Schott M, Willenberg HS, Scholl UI. *PRKACA* mutations in cortisol-producing adenomas and adrenal hyperplasia: a single-center study of 60 cases. Eur J Endocrinol 2015; 172:677-685

19. Espiard S, Knape MJ, Bathon K, Assié G, Rizk-Rabin M, Faillot S, Luscap-Rondof W, Abid D, Guignat L, Calebiro D, Herberg FW, Stratakis CA, Bertherat J. Activating *PRKACB* somatic mutation in cortisol-producing adenomas. JCI Insight 2018; 3

20. Chu C-S, Hsu P-H, Lo P-W, Scheer E, Tora L, Tsai H-J, Tsai M-D, Juan L-J. Protein Kinase A-mediated Serine 35 Phosphorylation Dissociates Histone H1.4 from Mitotic Chromosome. J Biol Chem 2011; 286:35843-35851

21. Shechter D, Dormann HL, Allis CD, Hake SB. Extraction, purification and analysis of histones. Nat Protocols 2007; 2:1445-1457

22. Safaei J, Maňuch J, Gupta A, Stacho L, Pelech S. Prediction of 492 human protein kinase substrate specificities. Proteome Sci 2011; 9:1-13
23. Bathon K, Weigand I, Vanselow J, Ronchi C, Sbiera S, Schlosser A, Fassnacht M, Calebiro D. Supplementary material for: Alterations in Protein Kinase A Substrate Specificity as a Potential Cause of Cushing's Syndrome. Figshare Digital Repository Deposited 29 August 2018. https://figshare.com/s/20c9287aefcd6b69f28d;
24. Cox J, Mann M. MaxQuant enables high peptide identification rates, individualized p.p.b.-range mass accuracies and proteome-wide protein quantification. Nat Biotech 2008; 26:1367-1372
25. O'Shea JP, Chou MF, Quader SA, Ryan JK, Church GM, Schwartz D. pLogo: a probabilistic approach to visualizing sequence motifs. Nat Methods 2013; 10:1211
26. Crooks GE, Hon G, Chandonia J-M, Brenner SE. WebLogo: A Sequence Logo Generator. Genome Res 2004; 14:1188-1190
27. Gibson RM, Taylor SS. Dissecting the Cooperative Reassociation of the Regulatory and Catalytic Subunits of cAMP-dependent Protein Kinase: role of Trp-196 in the catalytic subunit. J Biol Chem 1997; 272:31998-32005
28. Smith CM, Radzio-Andzelm E, Madhusudan, Akamine P, Taylor SS. The catalytic subunit of cAMP-dependent protein kinase: prototype for an extended network of communication. Prog Biophys Mol Biol 1999; 71:313-341
29. Lubner JM, Dodge-Kafka KL, Carlson CR, Church GM, Chou MF, Schwartz D. Cushing's syndrome mutant PKA^{L205R} exhibits altered substrate specificity. FEBS Lett 2017; 591:459-467
30. Fan YH, Nikitina T, Zhao J, Fleury TJ. Histone H1 depletion in mammals alters global chromatin structure but causes specific changes in gene regulation. Cell 2005; 123:1199-1212

31. Kim K, Choi J, Heo K, Kim H, Levens D, Kohno K, Johnson EM, Brock HW, An W. Isolation and Characterization of a Novel H1.2 Complex That Acts as a Repressor of p53-mediated Transcription. J Biol Chem 2008; 283:9113-9126

32. Izzo A, Schneider R. The role of linker histone H1 modifications in the regulation of gene expression and chromatin dynamics. Biochim Biophys Acta, Gene Regul Mech 2016; 1859:486-495

33. Gruneberg U, Neef R, Li X, Chan EHY, Chalamalasetty RB, Nigg EA, Barr FA. KIF14 and citron kinase act together to promote efficient cytokinesis. J Cell Biol 2006; 172:363-372

34. Faou P, Hoogenraad NJ. Tom34: A cytosolic cochaperone of the Hsp90/Hsp70 protein complex involved in mitochondrial protein import. Biochim Biophys Acta, Mol Cell Res 2012; 1823:348-357

35. Schmidt O, Harbauer AB, Rao S, Eyrich B, Zahedi RP, Stojanovski D, Schonfisch B, Guiard B, Sickmann A, Pfanner N, Meisinger C. Regulation of mitochondrial protein import by cytosolic kinases. Cell 2011; 144:227-239

36. Calebiro D, Bathon K, Weigand I. Mechanisms of Aberrant PKA Activation by Cα Subunit Mutations. Horm Metab Res 2017; 49:307-314

37. Fassnacht M, Hahner S, Hansen IA, Kreutzberger T, Zink M, Adermann K, Jakob F, Troppmair J, Allolio B. N-Terminal Proopiomelanocortin Acts as a Mitogen in Adrenocortical Tumor Cells and Decreases Adrenal Steroidogenesis. J Clin Endocrinol Metab 2003; 88:2171-2179

Figure legends

Fig. 1. Somatic *PRKACA* mutations identified in adrenal Cushing´s Syndrome. (A) Location of the identified *PRKACA* mutations in the crystal structure of the PKA holoenzyme. Note the clustering of the *PRKACA* mutations at the interface with the R subunit. The structure of the $RII\beta_2$:$C\alpha_2$ holoenzyme (Protein data bank/PDB entry 3TNP) was used as template. (B) Enlarged view of the PKA Cα-RIIβ interface. Shown are the positions of residues affected by *PRKACA* mutations relative to the inhibitory sequence of RIIβ in the PKA $RII\beta_2$:$C\alpha_2$ holoenzyme. The inhibitory sequence of RIIβ interacts with active site cleft of Cα and acts as a PKA substrate. Note the phosphorylated serine (S) residue within the canonical consensus for PKA phosphorylation (RRXS) in the inhibitory sequence. Most residues affected by *PRKACA* mutations participate directly or indirectly in substrate recognition. *, Residues affected by *PRKACA* mutations with largest predicted effects on substrate specificity based on *in silico* analysis. PDB entry 3TNQ was used as template.

Fig. 2. Effect of *PRKACA* mutations on the association of Cα with R subunits. HEK293A cells were co-transfected with FLAG-tagged RIIβ or RIα and either wild-type (WT) or mutant Cα subunits. The association between Cα and R subunits in the absence or presence of cAMP (200 μM) was analyzed by co-immunoprecipitation. Samples were immunoprecipitated (IP) with an anti-FLAG antibody, followed by Western blot analysis with an antibody against Cα. Western blot images were quantified by densitometric analysis. Data are mean±s.e.m. of three independent experiments. Arrows, mutants with conserved binding to R subunits. Differences are statistically significant by two-way ANOVA. *P<0.05, **P<0.01 and ****P<0.0001 vs. WT basal by Bonferroni´s post hoc test. Representative Western blot images are shown in Supplementary Data, Fig. 1 (23).

Fig. 3. Effect of *PRKACA* mutations on PKA activity against a synthetic substrate. HEK293A cells were co-transfected with RIα or RIIβ and either wild-type (WT) or mutant Cα subunits. PKA activity in cell lysates was then measured against an artificial peptide substrate (kemptide) in the presence or absence of cAMP (40 μM). The PKA activity measured in cells transfected with the empty expression vector (pcDNA) was subtracted. Data are mean±s.e.m. of three independent experiments. Data are statistically significant by two-way ANOVA. *P<0.05, ***P<0.001 vs. WT basal and $^{\#\#}$P<0.01, $^{\#\#\#}$P<0.001 vs. WT stimulated with cAMP by Bonferroni´s post hoc test.

Fig. 4. *PRKACA* mutations affect substrate specificity as revealed by phosphoproteomics analysis. HEK293A cells were co-transfected with RIIβ and either wild-type (WT) or mutant Cα subunits and labeled with light amino acids (WT) or heavy amino acids (mutant). Protein lysates from these cells were then proteolytically fragmented and the resulting phosphopeptides were immunoprecipitated using a phospho-PKA substrate antibody recognizing the RR/KXpS/T consensus. Phosphopeptides were separated and detected by nanoscale liquid chromatography coupled to tandem mass spectrometry (nano LC-MS/MS). Depicted are scatter plots showing the abundance of the detected phosphopeptides in the mutant relative to wild-type samples of three independent experiments. The sequence logos report, for each mutant, the relative amino acid preferences around the consensus motif (RR/KXpS/T) for both hypo- (left) and hyperphosphorylated (right) sequences, calculated from the phosphopeptides. Values are expressed as $\log_{10}$-odds of the significance of overrepresentation versus the significance of underrepresentation, which are calculated using the binomial probability of residue frequencies.

Fig. 5. Effect of *PRKACA* mutations on histone H1.4 phosphorylation in HEK293A cells. HEK293A cells were co-transfected with wild-type (WT) or mutant PKA Cα and the

RIIβ subunit. Histone H1.4 phosphorylation was probed by Western blot analysis with an antibody specifically recognizing H1.4 phosphorylated at Ser36. A Western blot analysis for total histone H.1.4 was used as loading control. Western blot images were quantified by densitometric analysis. The adenylyl cyclase activator forskolin (10 μM) was used to induce maximal PKA activity. Data are mean±s.e.m of three independent experiments. Differences are statistically significant by two-way ANOVA. *** P<0.001 vs. WT basal and # P<0.05 vs. WT forskolin by Bonferroni´s post hoc test.

Fig. 6. Effect of *PRKACA* mutations on histone H1.4 phosphorylation in tumor (CPA) samples from patients with adrenal Cushing´s syndrome. Histones were extracted from CPAs with or without *PRKACA* mutations and analyzed by Western blot analysis with an antibody specifically recognizing H1.4 phosphorylated at Ser36. A Western blot analysis for total histone H1.4 was used as loading control. Western blot images were quantified by densitometric analysis. Quantified data are mean±s.e.m of 3 and 4 CPAs carrying the L206R mutation or with *PRKACA* wild-type (WT), respectively. Differences are statistically significant by unpaired t-test (** P=0.009).

Table 1. List of somatic *PRKACA* mutations identified so far in CPAs of patients with overt Cushing's syndrome. Bold, studies by our group.

Tables

Mutation	Frequency (n mutated/total)	Reference
L206R	**36% (21/59)**	**(10)**
	60% (33/55)	(16)
	67% (84/126)	(14)
	35% (13/37)	(15)
	23% (3/13)	(17)
	34% (22/64)	**(11)**
	31% (11/35)	(18)
199_200insW	**2% (1/59)**	**(10)**
200_201insV	**5% (3/64)**	**(11)**
S213R+insIILR	**2% (1/64)**	**(11)**
W197R	**3% (1/39)**	**(12)**
d244-248+E249Q	**3% (1/39)**	**(12)**
E32V	**3% (1/39)**	**(12)**

Figures

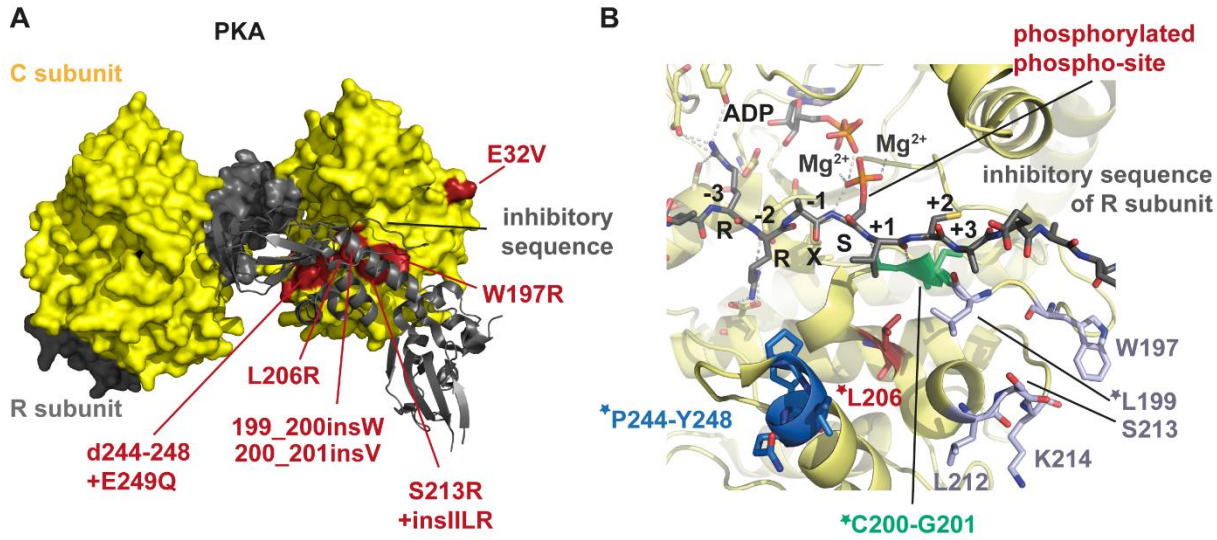

Fig. 1

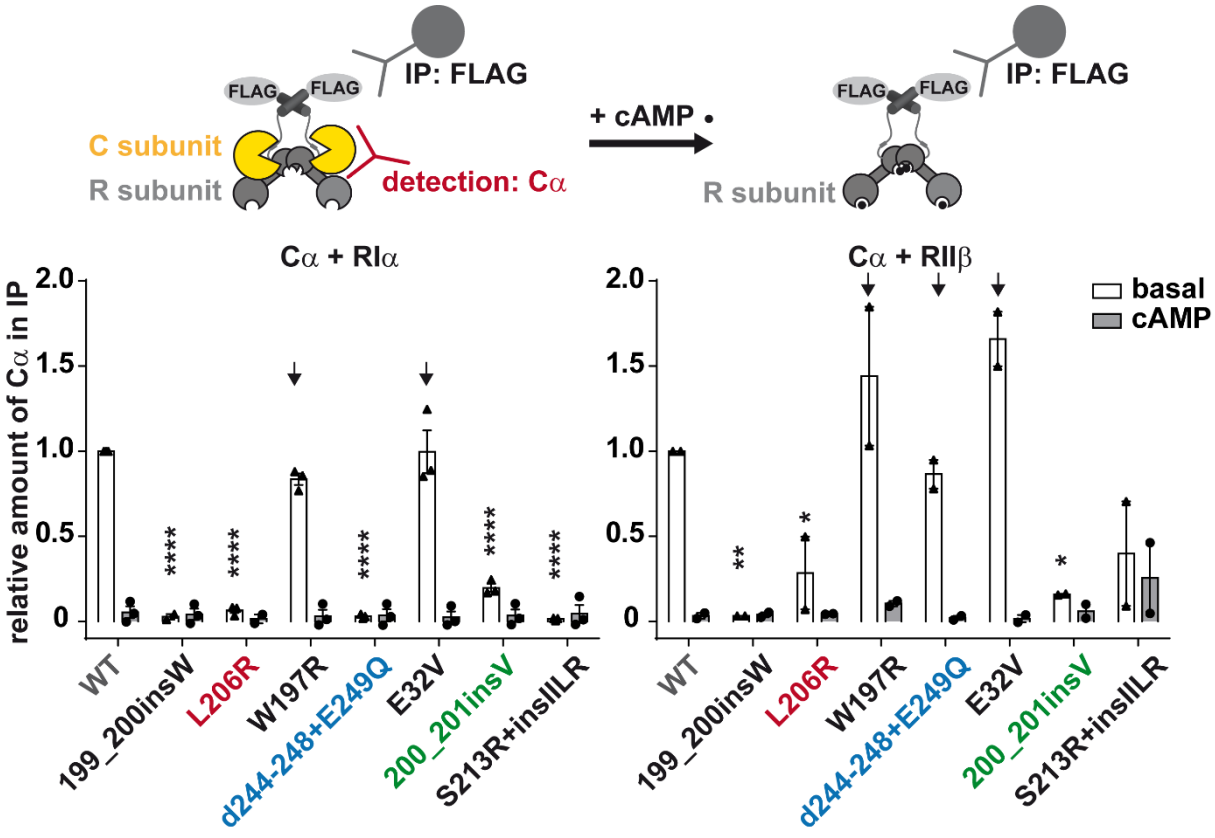
IP: FLAG
FLAG
FLAG
C subunit
R subunit
detection: Cα
+ cAMP
IP: FLAG
FLAG
FLAG
R subunit
Cα + RIα
Cα + RIIβ
basal
cAMP
relative amount of Cα in IP
2.0
1.5
1.0
0.5
0
WT
199_200insW
L206R
W197R
d244-248+E249Q
E32V
200_201insV
S213R+insIILR

Fig. 2

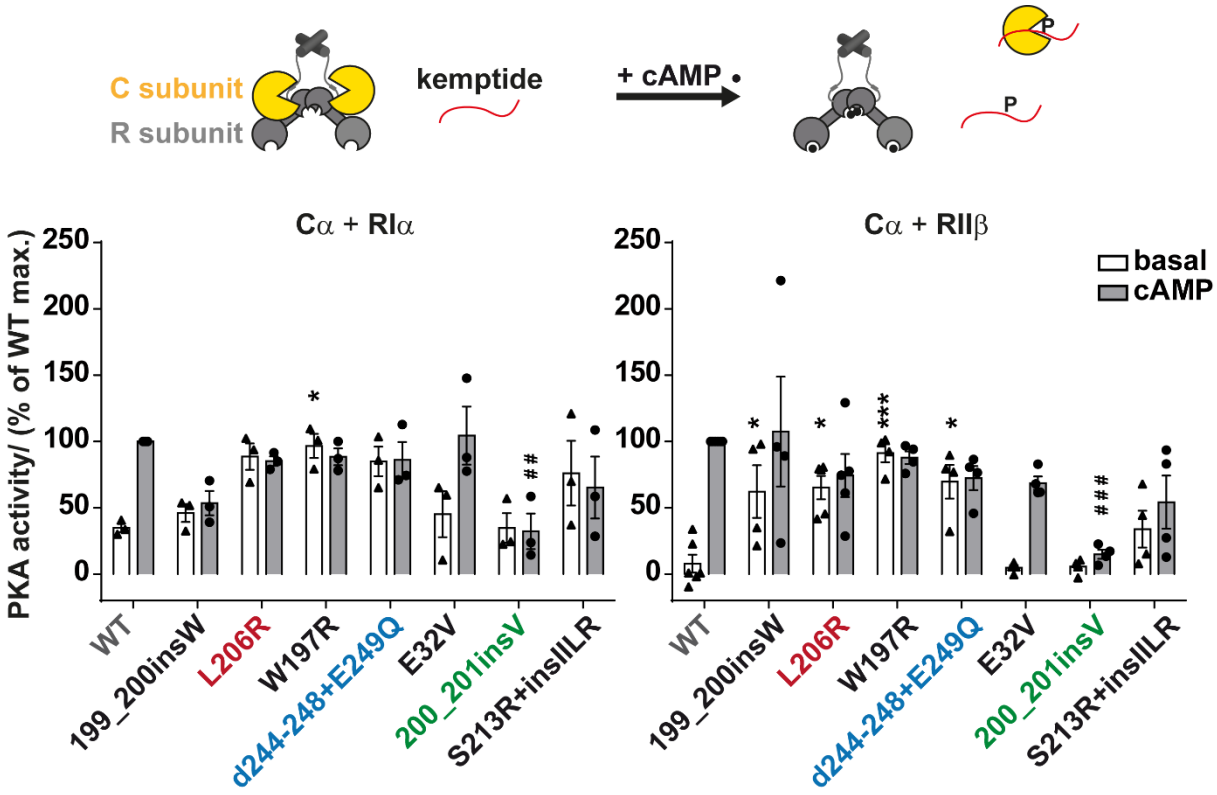
C subunit
R subunit
kemptide
+ cAMP
P
P
Cα + RIα
Cα + RIIβ
basal
cAMP
PKA activity/ (% of WT max.)
250
200
150
100
50
0
*
*
*
***
*
##
###
WT
199_200insW
L206R
W197R
d244-248+E249Q
E32V
200_201insV
S213R+insIILR

Fig. 3

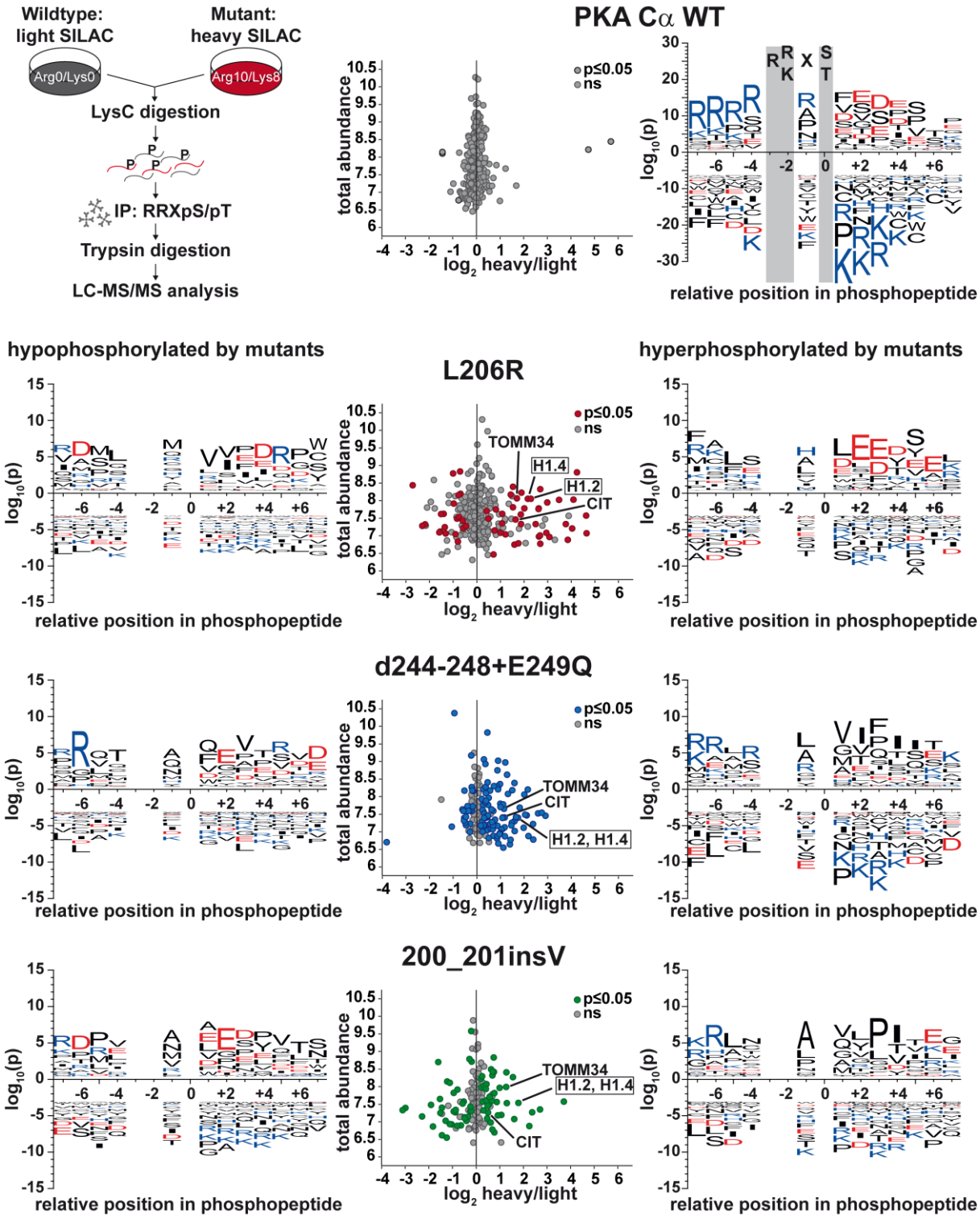
Wildtype:
light SILAC
Mutant:
heavy SILAC
Arg0/Lys0
Arg10/Lys8
LysC digestion
IP: RRXpS/pT
Trypsin digestion
LC-MS/MS analysis
PKA Cα WT
p≤0.05
ns
total abundance
log2 heavy/light
log10(p)
relative position in phosphopeptide
hypophosphorylated by mutants
hyperphosphorylated by mutants
L206R
TOMM34
H1.4
H1.2
CIT
d244-248+E249Q
H1.2, H1.4
200_201insV

Fig. 4

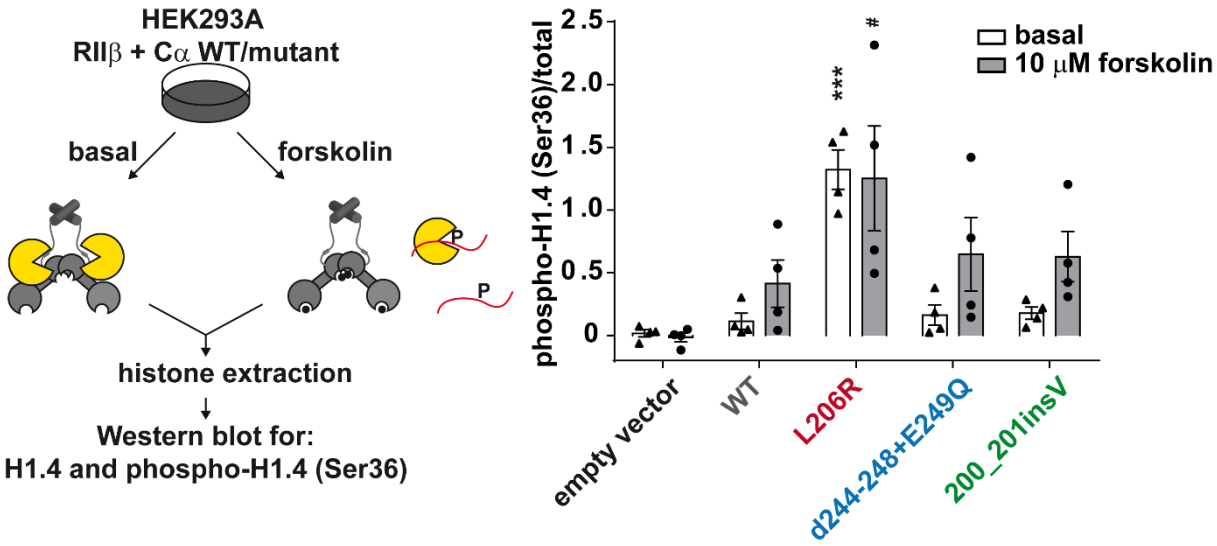
HEK293A
RIIβ + Cα WT/mutant
basal
forskolin
P
P
histone extraction
Western blot for:
H1.4 and phospho-H1.4 (Ser36)
phospho-H1.4 (Ser36)/total
2.5
2.0
1.5
1.0
0.5
0
***
#
basal
10 μM forskolin
empty vector
WT
L206R
d244-248+E249Q
200_201insV

Fig. 5

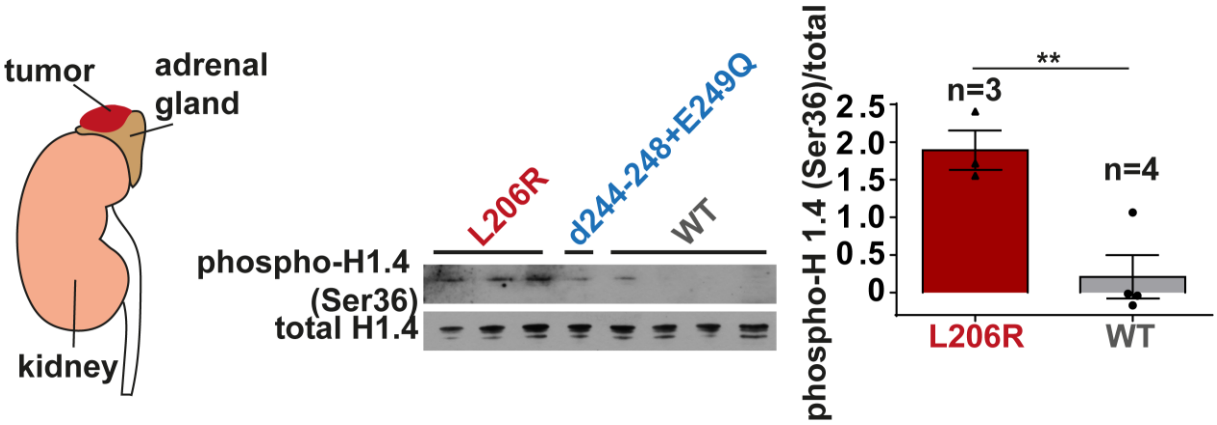
tumor
adrenal gland
kidney
L206R
d244-248+E249Q
WT
phospho-H1.4 (Ser36)
total H1.4
phospho-H 1.4 (Ser36)/total
2.5
2.0
1.5
1.0
0.5
0
**
n=3
n=4
L206R
WT

Fig. 6